# Enhanced Particle Filter framework for improved prognosis of Electro-Mechanical flight controls Actuators

Andrea De Martin[1], Giovanni Jacazio[2] and Massimo Sorli[3]

[1,2,3]*Politecnico di Torino, Torino, 10129, Italy.*

*andrea.demartin@polito.it*
*giovanni.jacazio@polito.it*
*massimo.sorli@polito.it*

## ABSTRACT

Flight Control Systems (FCSs) are one of the most interesting field of research and application for Electro Mechanical Actuators (EMAs), which are theoretically able to provide several advantages over the traditional hydraulic/mechanical solution for both primary and secondary flight control surfaces. However, in particular when compared to hydraulic actuators, technological barriers for a wide adoption of EMAs still persist, especially when considering their sensitivity to certain single point of failures that can lead to mechanical jams. As such, EMAs are so far not employed for flight safety critical applications as solutions are heavy and costly (redundancy, fail safe behavior, etc.), while their certification is made more difficult due to the additional design complexity. The development of an effective and reliable PHM system for EMAs could help in mitigating the risk of a sudden critical failure by properly recognizing and tracking the on-going fault and anticipating its evolution, thus offering a possible boost to the acceptance of EMAs as primary flight control actuators in commercial aircraft. The paper firstly presents an enhanced Particle Filter framework for improved prognosis, discussing its benefits and its implementation inside a general PHM framework developed for EMAs. Further developing on previously published works, three degradation modes are hence identified as significant and used as case study. The first one is the degradation of the magnets of the electric motor, associated with dynamic performance losses and decrease of the stall load. The other two are the increase of the backlash in the mechanical transmission due to the growing wear of its components, as well the wear of the spherical joints connecting the actuator to the surface (rod-end). The positive results obtained from the application of the enhanced Particle Filtering framework to these faults provide good confidence on the possibility of extending it to other EMAs faults and to successfully implement this technique to EMAs for flight control actuators.

## 1. INTRODUCTION

The Electro-Mechanical Actuators (EMAs) technology has been object of several research programmes for FCS in the recent years; EMAs are in fact able to provide several advantages over the traditional Electro-Hydraulic and even the novel Electro-Hydrostatic Actuators by eliminating leakage problems, simplifying the installation and the maintenance operations while keeping the overall weight competitive (Pratt, 2000). Their application on civil aircrafts is however severely limited by safety issues associated with single point failures, making them far more suitable for experimental vehicles and UAVs (Jensen, Jenney & Dawson, 2000), (Derrien, Tieys, Senegas & Todeschi, 2011), (Roemer & Tang, 2015). EMAs have found some applications on non-safe critical control surfaces such as flap/slats control (Christmann, Seemann & Janker, 2010), (Recksieck, 2012). A possible solution to these safety issue is to study and apply a robust PHM system able to rapidly detect the insurgence of dangerous fault conditions and to anticipate their evolution into full-blown failures. Several research efforts can be found in specialized literature, addressing the electric motor (Nandi, Toliyat & Li, 2005), (Brown and others, 2009), (Belmonte, Dalla Vedova & Maggiore, 2015), and (De Martin, Jacazio & Vachtsevanos 2017), mechanical components (Balaban, Saxena, Goebel, Byington, Watson and others, 2009), (Balaban, Saxena, Narasimhan, Roychoudhury & Gobel, 2010) and (Lessmeier, Enge-Rosenblatt, Bayer & Zimmes, 2014) and electronic power unit (EPU) (Brown, Abbas, Ginart, Ali, Kalgren, Vachtsevanos, 2010), (Li, Ye, Chen, Vachtsevanos, 2014). Many of the presented studies make use of Particle Filtering frameworks to perform the failure prediction and Remaining Useful Life (RUL) estimate. The research presented in this work introduces a novel declination of this technique specifically studied for FCS applications to tackle the most prominent issues associated

with the Health Monitoring of these devices. After a brief introduction on such practical issues, we present the framework and its expected benefits; hence we present a case study based on a flight control surface moved by two EMAs in active-active configuration and compare the results with that obtainable though a traditional particle filter.

## 2. PROMINENT ISSUES IN PHM FOR FLIGHT CONTROLS

The field of Flight Control Systems (FCSs) is an extremely interesting application for PHM technologies, in particular that of primary flight control actuators; these devices provides a significant challenge for PHM techniques, since they are safety critical, behave following command patterns difficult to predict a-priori and their actuation time is limited through most of the mission. The development of robust PHM techniques would allow to mitigate the safety issues, enhancing the aircraft availability and eventually affecting the design of the actuators, enabling new technologies (such as the EMAs) or novel architectures. At the same time, FCS applications could be considered as a benchmark for PHM techniques due to a few intrinsic issues that hamper the feature selection and further complicate the design of a comprehensive Health Monitoring system. The first and most prominent issue is the uncertainty associated with the features computed from signals coming from in-flight measures. The operational conditions can be widely varying, the aerodynamic load pattern is often unpredictable due to gusts and turbulence and so are the pilots commands, which are influenced by the pilot performances, contingent flight situation etc. The effects of this uncertainty are further expanded by other issues, such as the low number of signals available and the absence of direct measures of important quantities such as the aerodynamic load. Vibration measures are moreover made difficult by the short duration of each actuation and by the rarity of the occurrence of steady-state conditions. Finally, local measures that would be instrumental for PHM are often difficult to make, in particular for legacy equipment. To address these issues, Jacazio, Maggiore, Della Vedova, and Sorli (2010) proposed the use of dedicated pre or post flight checks based on short, repeatable sequences of commands studied to enhance the effects of a selected number of faults over the available signals. This approach has the significant advantage of extracting the features in a semi-controlled environment, (negligible external load, pre-defined commands) while allowing for sequences of movements that cannot be performed in flight; this becomes particularly interesting for flight control surfaces controlled by at least two actuators, since it would allow to use one of the actuators to impose a known load on the other, enhancing the effects of certain fault types (Mornacchi, Jacazio & Vachtsevanos, 2015), (De Martin, Jacazio & Vachtsevanos, 2016). At the same time, a significant drawback is represented by the time scarcity of the obtainable data, since

only one acquisition per mission is possible; this makes it difficult to perform an efficient failure prognosis and does not allow to address degradations which last less than the duration of a single mission. A possible solution to these issue could be the definition of a framework able to combine the noisy but frequently available information obtainable in-flight with the more accurate ones coming from dedicated pre-flight test.

## 3. PARTICLE FILTER FOR FAILURE PROGNOSIS

PHM frameworks are based on three consecutive steps, which are,

- Signal conditioning and feature extraction
- Fault diagnosis (detection/identification/isolation)
- Failure prognosis

Once an incipient failure or fault is detected through proper algorithm with a specified confidence, the prognostic algorithm is initiated to predict the fault's time evolution. The fault state at detection acts as the initial condition for the prognosis, which framework is depicted in Fig. 1. The prognostic framework is based on a nonlinear degradation model and a Bayesian estimation method using particle filtering and real-time measurements (Vachtsevanos and others, 2006) to perform failure prognosis under general assumptions of non-Gaussian noise structures and nonlinearities in process dynamic models using a reduced particle population to represent the state probability density function (pdf). A complete overview of the Particle Filter theory can be found in (Orchard, 2007). The particle filter-based module is built upon the nonlinear dynamic state model,

$$\begin{cases} x(t) = f_t\big(x_d(t), x(t-1), \omega(t)\big) \\ y(t) = h_t\big(x_d(t), x(t), v(t)\big) \end{cases} \quad (1)$$

where $f_t$ and $h_t$ are non-linear mappings, $x_d$ is a collection of Boolean states associated with the presence of a particular operating condition in the system (normal operation, fault type #1, #2, etc.), $x$ is a set of continuous-valued states that describe the evolution of the system given those operating conditions (i.e. fault size). We address with $y$ the feature measurement, $\omega$ and $v$ are non-Gaussian distributions that characterize the process and feature noise signals, respectively.
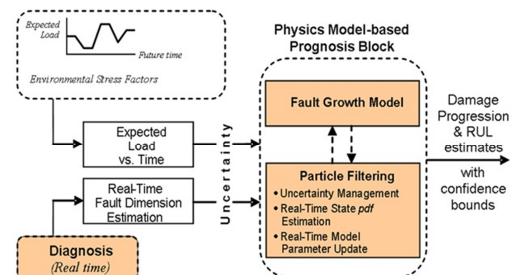


Figure 1. The Prognostic Framework

The function $h_t$ is a mapping between the feature value, $y(t)$, and the fault state $x(t)$. Prognosis is achieved through particle filter, which works by performing two sequential steps, prediction and filtering. Prediction uses both the knowledge of the previous state estimate $x_{t-1}$ and the process model $\omega(t)$ to generate the a priori state pdf estimate for the next time instant,

$$p(x_{0:t}|y_{1:t-1}) = \int p(x_t|y_{t-1})p(x_{0:t-1}|y_{1:t-1}) \, dx_{0:t-1} \qquad (2)$$

Unfortunately, this expression does not have an analytical solution in most cases. Sequential Monte Carlo (SMC) algorithms, or particle filters, are hence used to numerically solve this equation in real-time with efficient sampling strategies (Bishop, 2006). Particle filtering approximates the state pdf using samples or "particles" having associated discrete probability masses ("weights") $\widetilde{w}_t$,

$$p(x_t|y_{1:t}) \approx \widetilde{w}_t(x_{0:t}^i)\delta(x_{0:t} - x_{0:t}^i)dx_{0:t-1} \qquad (3)$$

where $x_{0:t}^i$ is the state trajectory and $y_{1:t}$ are the measurements up to time $t$. The simplest implementation of this algorithm, the Sequential Importance Re-sampling (SIR) particle filter, updates the weights using the likelihood of $y_t$ as

$$w_t = w_{t-1}p(y_t|x_t) \qquad (4)$$

Long-term predictions are used to estimate the probability of failure in a system given a hazard zone that is defined via a probability density function with lower and upper bounds for the domain of the random variable, denoted as $H_{lb}$ and $H_{up}$, respectively. The probability of failure at any future time instant is estimated by combining both the weights $w_{t+k}^{(i)}$ of predicted trajectories and specifications for the hazard zone through the application of the Law of Total Probabilities.

The resulting RUL pdf, where $t_{RUL}$ refers to RUL, provides the basis for the generation of confidence intervals and expectations for prognosis,

$$\hat{p}_{t_{RUL}} = \sum_{i=1}^{n} p\big(\text{Failure}|X = \hat{x}_{t_{RUL}}^{(i)}, H_{lb}, H_{up}\big) \qquad (5)$$

## 4. ENHANCED PARTICLE FILTER FRAMEWORK

The Enhanced Particle Filter Framework depicted in Fig. 2 has been built to improve its prognostic performances by

- Adapting the non-linear mappings through continuous stream of data
- Reducing the effect of noise propagation for the long-term prediction stage
- Using the more accurate data obtainable during pre-flight tests to periodically check and correct the state estimates performed through in-flight data

The first objective is realized by auto-tuning the non-linear mappings (1) through Recursive Least Square algorithm, which has the benefit of being computationally inexpensive and hence well-suitable for on-line applications. Another possible solution, implemented in the code but not shown in this paper, has been recently proposed by Echauz, Gardner, Curtin, Vasiloglou and Vachtsevanos (2017), that is based on the use of parallel pools of Particle Filters to pursue a more robust statistical characterization of the non-linear models at the expense of computational efficiency. To reduce the effect of noise propagation we resort to an approach derived from Orchard (2007), where the noise $\omega$ applied to each iteration of the degradation model is modified through the coefficient $(1 + K_\omega)$, obtained as the
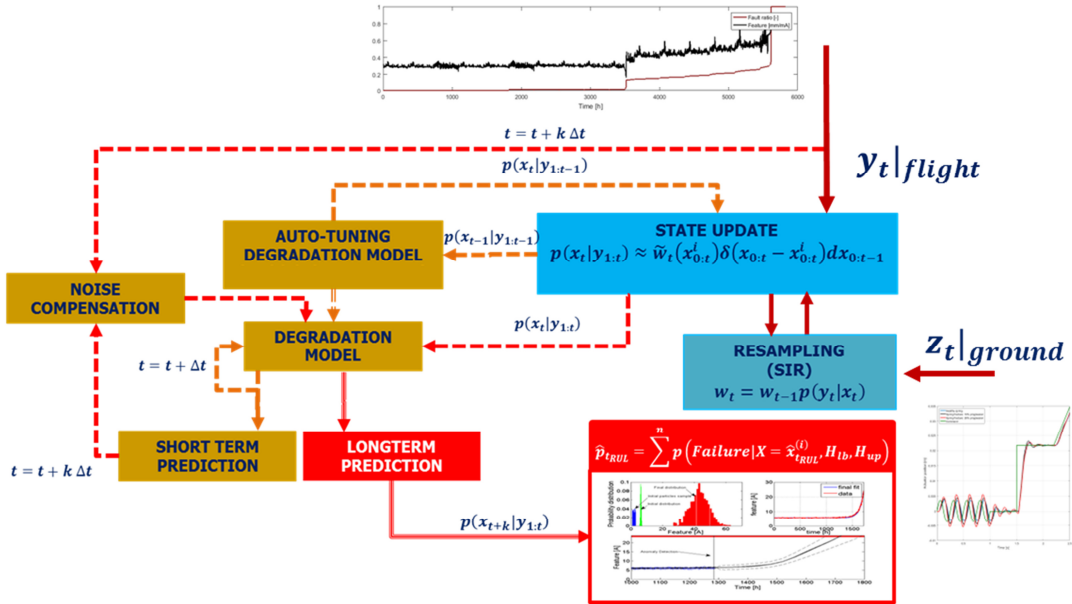


Figure 2. The Enhanced Particle Filter Framework

time integral of the difference between the noise behaviour of the estimated states and of the projected states computed as,

$$K_\omega = K_I \int_t [var(x_{t+\Delta T}) - var(\hat{x}_{t+\Delta T})]\, dt \qquad (6)$$

where $var(\hat{x}_{t+\Delta T})$ is the variance of the projected particles $\hat{x}$ obtained projecting the states estimate $x$ at time $t$ for a number of iterations corresponding to a time step equal to $\Delta T$, while $var(x_{t+\Delta T})$ is the variance of the states' estimate at time $t + \Delta T$. The introduction of the on-ground measures is finally performed by adding to the non-linear mappings of Eq. (1) the non-linear model linking the on-ground observations $z$ with the states $x$

$$z(t) = g_t\big(x(t), \varphi(t)\big) \qquad (7)$$

where $\varphi$ is non-Gaussian noise. The model is hence used along the on-ground observations (when available) to update the weights of the Particle Filter as,

$$w_t = w_{t-1} p(y_t|x_t) p(z_t|x_t) \qquad (8)$$

## 5. CASE STUDY

We focus on the most general scheme for primary flight control surfaces moved by two EMAs represented in Fig. 3. Each of the two EMAs is made of one brushless electric motor (EM) supplied through its own Electronic Power Unit and a mechanical transmission made of a satellite gearbox (GB) and a roller screw. The position control of each actuator is performed through three nested loops, which modulate the electric motor currents, the driving shaft speed and the linear position of the screw. Feedback signals are generated by current sensors, a resolver positioned on the motor shaft and LVDTs, connected to the translating element of the power screw. The position command is provided by two inter-communicating Flight Control Computers (FCCs) which generate the control signal following the active/active strategy, which means that both devices are contemporary actuated in position while receiving the same command input. This control strategy allows to obtain better dynamics response and to limit the usage of each motor, but is prone to force fighting, which occurrence causes one of the actuators to apply a resistant load that must hence be compensated by the other. This phenomenon usually happens when the aerodynamic load acting on the system is almost null and it's due to the inevitable deviation from the nominal value of some of the actuators characteristics, such as friction behavior, backlashes, inertia and motor parameters. It may lead to windings overheating and generally shortens the motor operative life. Force fighting can be compensated by motor current equalization, as in the system under analysis, or by monitoring the force exerted by each actuator using proper transducers and a dedicated controller working either on the position or on the speed loop (Wang, Maré, Fu, 2012).
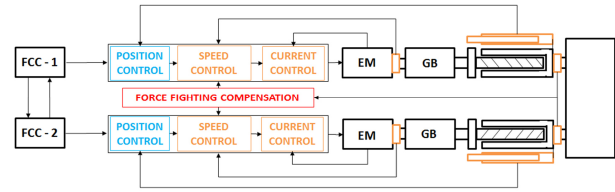


Figure 3. EMA configuration

For this architecture, authors already discussed both on-ground and in-flight implementation of PHM techniques for windings faults in (De Martin, Jacazio and Vachtsevanos, 2016) and (De Martin, Jacazio and Vachtsevanos, 2017). The presented paper is instead focused on two other common fault processes of EMAs for FCS applications, such as the permanent magnets degradation in the electric motor and the backlash increase due to wear progression in the mechanical transmission and in the rod-end. By updating the FMECA provided in (De Martin, Jacazio and Vachtsevanos, 2016) and here reported in Table 1, we can rank the possible failure modes in occurrence Frequency (F), effects Severity (S), feature Traceability (T) and component Replaceability (R), with lower scores addressing the more critical conditions. The most critical between the three cases is the rod-end wear, which may cause loss of positioning accuracy and dynamic stiffness, associated with increasing oscillations of the aerodynamic surface.

Table 1. FMECA results

| COMPONENT | MAIN FAILURE MODES | SCORE | | | | |
|---|---|---|---|---|---|---|
| | | F | S | T | R | TOT |
| EPU | Base-drive open circuit | 3 | 2 | 4 | 1 | 10 |
| Electric motor | Turn-to-turn short | 1 | 2 | 4 | 1 | 8 |
| | Magnets degradation | 3 | 2 | 3 | 1 | 9 |
| Bearings | Scoring | 3 | 1 | 3 | 1 | 8 |
| | Indentation | 4 | 1 | 3 | 1 | 9 |
| | Wear | 4 | 4 | 3 | 1 | 12 |
| | Pitting | 4 | 4 | 3 | 1 | 12 |
| | Electric erosion | 3 | 2 | 3 | 1 | 9 |
| | Tracks crack | 3 | 1 | 3 | 1 | 8 |
| Gears | Crack | 3 | 1 | 3 | 1 | 8 |
| | Wear | 2 | 3 | 3 | 1 | 9 |
| | Pitting | 2 | 3 | 3 | 1 | 9 |
| Power screw | Scoring | 2 | 1 | 3 | 1 | 7 |
| | Wear | 2 | 3 | 3 | 1 | 9 |
| | Return channel deformation | 4 | 1 | 3 | 1 | 9 |
| | Indentation | 3 | 1 | 3 | 1 | 8 |
| Rod-end | Wear | 2 | 2 | 3 | 1 | 8 |
| | Crack | 4 | 1 | 2 | 1 | 8 |
| | Rod deformation | 4 | 1 | 2 | 1 | 8 |

### 5.1. System model

Lacking of an experimental set-up, we resorted to a high-fidelity model of the system, implemented in

Matlab/Simulink and interfaced with the PHM routines. The EPU/brushless motor model have been modeled as a three-phase system with Field-Oriented-Control (FOC) according to the approach proposed by (Mohan, 2003) and (Hanselman, 2006), which neglects the MOSFET dynamics in the EPU and concentrate the electrical dynamics in the motor windings.

$$\begin{bmatrix} v_a \\ v_b \\ v_c \end{bmatrix} - \frac{d}{dt}\begin{bmatrix} \lambda_a \\ \lambda_b \\ \lambda_c \end{bmatrix} = \begin{bmatrix} R_a & 0 & 0 \\ 0 & R_b & 0 \\ 0 & 0 & R_c \end{bmatrix}\begin{bmatrix} i_a \\ i_b \\ i_c \end{bmatrix} + \frac{d}{dt}\left(\begin{bmatrix} L_{aa} & L_{ab} & L_{ac} \\ L_{ab} & L_{bb} & L_{bc} \\ L_{ac} & L_{bc} & L_{cc} \end{bmatrix}\begin{bmatrix} i_a \\ i_b \\ i_c \end{bmatrix}\right) \quad (9)$$

Where the three phase voltages $v_{a,b,c}$ are function of the MOSFET switch state $q$. $R_i$ and $L_i$ are the electric resistance and inductance for the i-th phase, while $\lambda_i$ is the concatenated flux. Given the pair poles number, the electromagnetic torque can be obtained, while the windings' temperature is evaluated through the a simplified mono-dimensional heat exchange dynamic model. The mechanical transmission has been modelled to include a non-linear friction law and a customizable elasto-backlash following the approach proposed by (Nordin, Gallic, Gutman, 1997). Each mechanical element is described through its dynamic equilibrium equation, while torque disturbances due to imperfect gearing have been over imposed at the meshing frequency. The friction law has been approximated through non-linear equations depending on temperature, speed and applied load. The aerodynamic surface has been modelled as a system of parallel springs and dampers, as shown in Figure 4. The aerodynamic force $F_A$ is function of the aircraft speed and of the tab positioning, plus a random load which rare occurrence is used to simulate the effect of gusts.
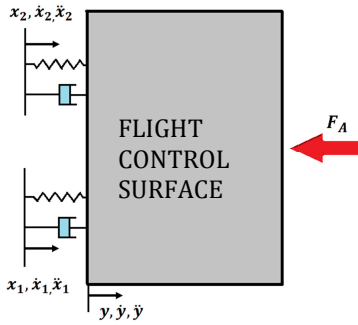


Figure 4. Control surface scheme

### 5.2. Degradations model

The degradations have been implemented in the model as

- a progressive decrease of the magnetic flux (magnets degradation)
- progressive increase of the size of the elasto-backlash within the screw and the nut, as well as in the rod-end

The magnets degradation follows the evolution described in (Ruoho, Dlala & Arkkio, 2007), which links the progressive loss of residual magnetization with the rotor temperature and the load cycle. We address in this paper a

uniform degradation of the magnetic properties of the magnetic poles pairs, meaning that each pair pole degrades in the same way and with the same, or only slightly different, evolution in time. This kind of degradation does not create any asymmetry in the motor currents, that may instead be caused by shorts in the motor windings (De Martin, Jacazio and Vachtsevanos, 2016), non-uniform degradation of the magnet or failures in the EPU (Celaya, Saxena, Wysocki, Saha, Goebel, 2010). An example of the effect of this degradation on the motor currents in absence of external load is reported in Fig. 5. The wear in the mechanical transmission evolves according to Archard's Law (1953), which relates the wear ratio to the relative speed of the mating bodies and the contact force. Both the relative speed and the contact force are obtained imposing realistic histories of loads and commands to the simulated system. An example of the effect of the wear increase over the EMAs behavior is shown in Fig. 6.
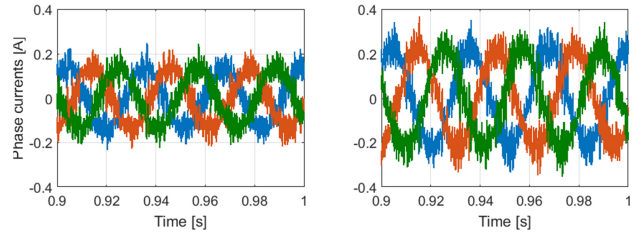


Figure 5. Effect of uniform magnets degradation on phase currents: healthy (left) degraded (right)
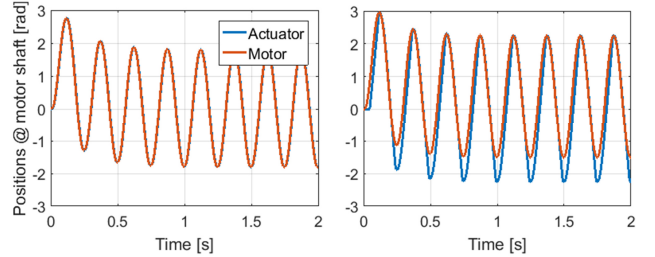


Figure 6. Effect of uniform wear in the screw: healthy (left) severe degradation (right)

### 6. PHM FRAMEWORK

In the following paragraph we present the PHM framework implementation and the role of the Enhanced Particle Filter.

### 6.1. PHM strategy

In absence of reliable information on the aerodynamic load, the proposed feature for the uniform degradation of the permanent magnets has been defined as,

$$f_{DMD} = \frac{RMS(v_{a,b,c})}{|\omega_m|} \quad (10)$$

Where $V_{a,b,c}$ are the phase voltage and $|\omega_m| \neq 0$ is the absolute value of the rotational speed of the brushless motor. The feature has been chosen from a short list of

candidates according to correlation and accuracy measure criteria. This feature has the benefit of being relatively inexpensive to compute and only reliant on the available sensors, being hence suitable for on-line operation. However it can become quite noisy, since it intrinsically depends on the mechanical efficiency of the transmission, function of the temperature, humidity and wear conditions. As such, we propose its use in combination with the following pre-flight check,

- Actuator 1 is active and commanded along a position ramp corresponding to at least 5 electric periods of the motor.

- Actuator 2 is not supplied and is hence moved by actuator 1. The measured phase voltages are then directly associated with the back-electromotive force and hence with the magnets behavior

The procedure is repeated switching the roles of the two actuators. The observation of the effect of wear in the mechanical components during flight is made difficult by the significant uncertainty associated with the combined effect of commands and loads direction. The quantization error and the resolution of the digital acquisition system for the position signals has to be considered as well. In principle, we can think to observe the increasing backlash in the mechanical transmission as,

$$ b \approx \left| \vartheta_m - \left( \tau_{gb} \frac{2\pi}{p_{rs}} \right) x_s \right| \qquad (11) $$

where $\vartheta_m$ and $x_s$ are the position signals coming from the resolver mounted on the motor axis and from the LVDTs integral with the screw; $\tau_{gb}$ is the gearbox transmission ratio

and $p_{rs}$ the screw's step. It must be stressed that the most significant contribute to the value of $b$ comes from the latter stages of the gearbox and the screw. As such, advancing wear in the first stage of the gearing might be overlooked. Another possibility is represented by the study of the motors currents behavior in the transients, which have the downside of being possibly affected by a high number of electrical faults. In this case we hence propose to combine the measures obtained from Eq. (11) with the following pre-flight check procedure,

- Actuator 1 is active and commanded along a 2Hz sinusoid of position.

- Actuator 2 is not supplied and is hence moved by actuator 1.

We hence estimate the backlashes $b_1$ and $b_2$ in the two actuators as the average of the four peaks obtained by applying Eq. 11. Moreover, we can also estimate the overall backlash on the spherical joints as the average of the four peaks of

$$ b_{re} = \left| \vartheta_{m,1} - \vartheta_{m,2} \right| - \left| b_1 + b_2 \right| \qquad (12) $$

The two pre-flight tests here presented can be united in one comprehensive command sequence, composed of the sinusoid and the ramp. Each of the presented features have been chosen based on correlation and accuracy criteria out of a pool of other candidates.

### 6.2. Fault diagnosis

The first step of the PHM framework is to perform the fault detection and hence its isolation/identification to complete the diagnosis. The anomaly detection is performed
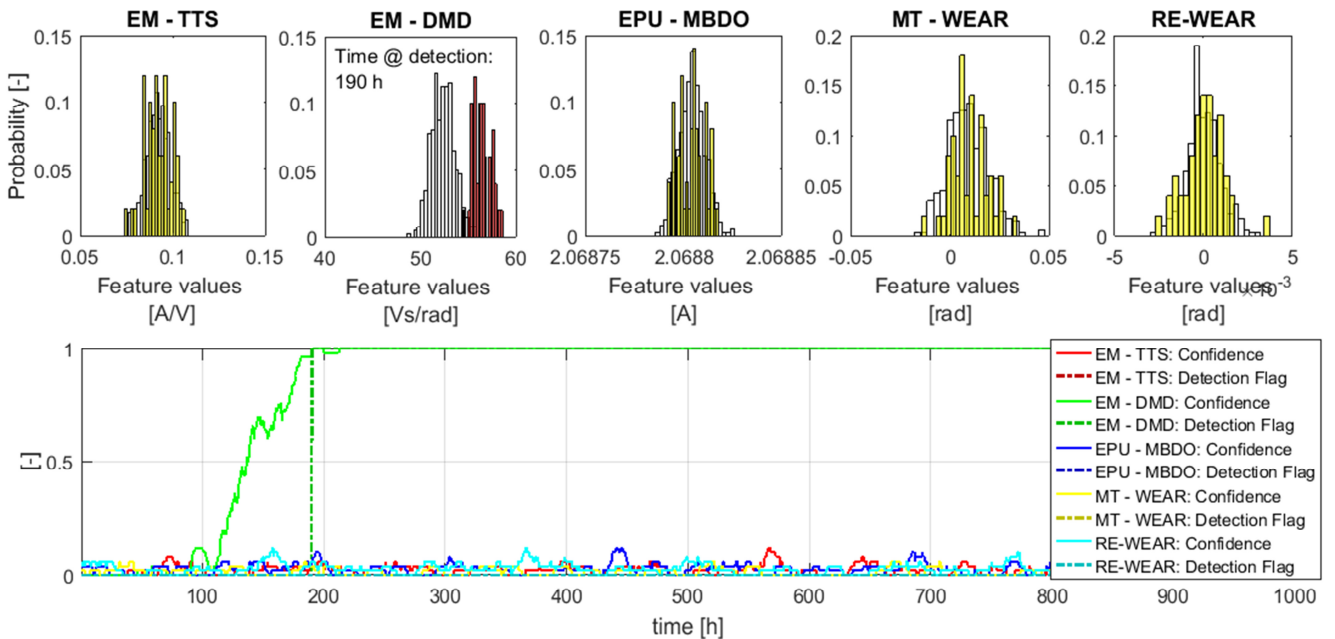


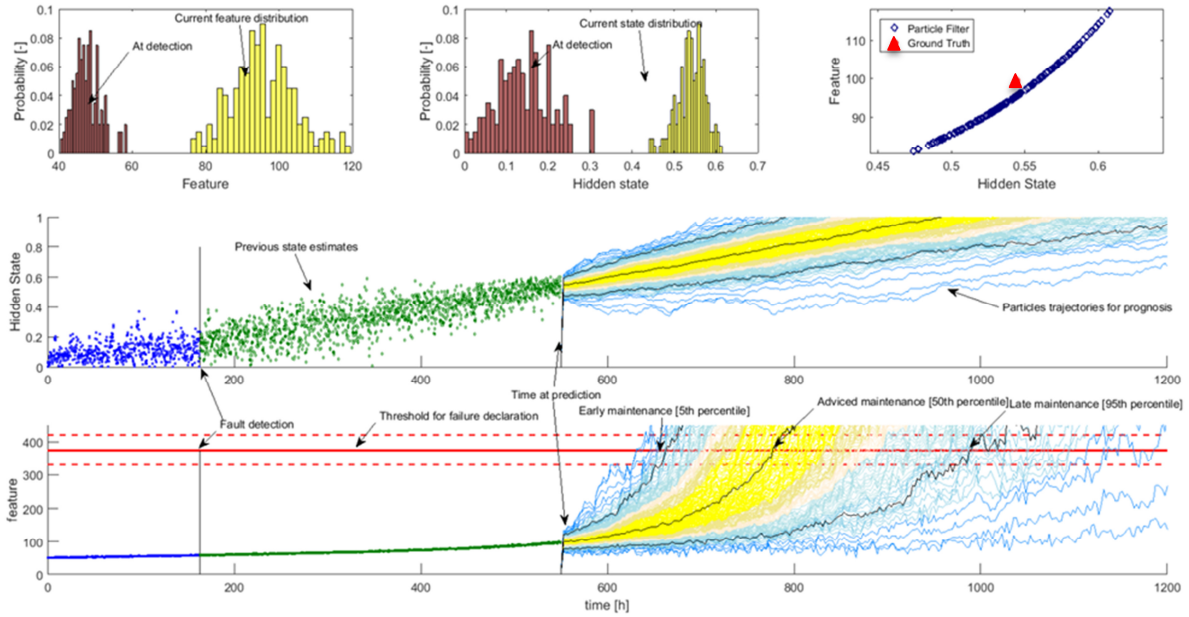Figure 7. Fault detection output for degradation of the motor magnets

Figure 8. Prognosis for magnets degradation

through a simple data-driven method, which compares the moving distribution of probability of each feature with their baseline distributions obtained for healthy conditions. The condition for the fault declaration is that at least 95% of the moving distribution overcomes the 95$^{th}$ percentile of the related baseline. In this way, we can define a-priori the type-I and type-II errors (Vachtsevanos et al., 2006). In Fig.7 it is reported an example of the results of the anomaly detection routine; for each actuator we observe the behavior of the features associated with the turn-to-turn short in the motor (code: EM-TTS) (De Martin, Jacazio and Vachtsevanos, 2017), the magnets degradation (code: EM-DMD), MOSFET base-drive open circuit issues in the EPU (EPU-MBDO), wear inside the mechanical transmission (code MT-WEAR) and in the rod-end (RE-WEAR). When the onset of a fault progression is detected, the features values, normalized between 0 and 1, are sent to an Artificial Neural Network which performs the classification. The selected features are characterized by low values of correlation with other classes, meaning that their behavior is significantly affected only by one of the selected fault process. As such, fault classification is straight-forward and no misclassifications have been recorded. The system is able to recognize the occurrence of magnets degradation within the 12.3% of its growth, while the fault percentage at detection for the wear progression is 8.5% in average for the mechanical transmission and 8.5% for the rod-end.

## 6.3. Failure prognosis

The failure prognosis is performed applying the enhanced Particle Filter presented in section 4. Data for this stage have been obtained by applying the models presented in section 5.2 under realistic profiles of command, loads and temperature conditions. The thresholds for each feature are defined as the 50$^{th}$ percentile of their distribution in correspondence of the final failure conditions. An example of the prognostics framework output for the demagnetization fault mode is reported in Fig. 8, where we can observe the probability distributions associated with the feature values and the estimated fault size (hidden state) in correspondence of the fault detection and of the prediction instants. For each prediction, three values of RUL are estimated, each associated with a different confidence levels (traditionally 5%, 50% and 95%). We address each of these RUL estimates as "early maintenance", "advised maintenance" and "late maintenance". These three values tends naturally to convergence toward the latest stages of the fault evolution. Traditionally, the reference RUL is the one associated with the 50% confidence. To each anomalous condition corresponds a different Particle Filter call and hence a different RUL estimate.

## 6.4. Performance assessment and discussion

Prognosis performance has been analyzed through the state-of-the-art metrics proposed by Saxena, Celaya, Balaban, Goebel, Sasha and Schwabacher (2008), namely the $\alpha$–$\lambda$ analysis, the Relative Accuracy (RA) and the Cumulative Relative Accuracy (CRA).

The $\alpha$–$\lambda$ analysis, hereby reported in non-dimensional form, is used to graphically describe the convergence of the RUL estimate to the ground truth RUL. On the abscissa, time is reported as $\lambda$ in non-dimensional form with respect to the component End Of Life (EOL), while on ordinate it is reported the ratio between the RUL and the real RUL (RUL$_r$) at fault detection. Tolerance bands, usually

correspondent to $\pm20\%$, are depicted as well. Through the $\alpha-\lambda$ it is possible to identify the Prognostic Horizon (PH) of the system for the investigated fault mode, that is the first real RUL value for which the prognosis falls within the afore-mentioned tolerance bands. The Relative Accuracy is defined as in Eq. (13), where its mean value is used to assess the average accuracy of the prediction framework:

$$RA = 1 - \frac{|RUL_r - RUL|}{RUL_r} \qquad (13)$$

The Cumulative Relative Accuracy is instead used to assess the behavior of the prognostic framework giving higher importance to the predictions performed when near to the EOL. This is achieved by a weighted sum of the RA computed at several prediction instants, where the weights are often the values of λ:

$$CRA = \frac{1}{\sum_i \lambda_i} \sum_i \lambda_i \, RA_i \qquad (14)$$

The $\alpha-\lambda$ analysis for the selected fault modes (magnets degradation, wear in the mechanical transmission and wear in the spherical joints of the actuator rod-end) are reported in Figs. 9, 10 and 11. The Prognostic Horizon for the magnets degradation is up to more than 240 hours for the case under examination; the average RA, computed over 20 equally spaced predictions, is 87.85% and the CRA is 90.18%. For the wear in the mechanical transmission, the Prognostic Horizon for the magnets degradation is up to more than 760 hours for the case under examination; the average RA, computed over 20 predictions, is 90.05% and the CRA is 81.02%. Finally, for the wear in the spherical joints of the actuators rod-ends, the Prognostic Horizon is 680 hours circa; while the average RA, is 72.47% and the CRA is 82.03%. Please notice that, while the average RA value is low if computed over the whole range of operation of the prognostic framework, the achieved prognostic horizon is still high. The low value of the mean RA is hence due to the system lack of accuracy during the first stages of
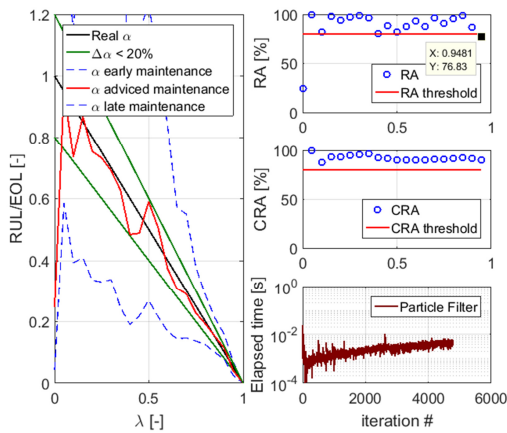
the fault progression which, according to van den Bossche (2009), can be extremely lengthy (up to $10^4$ flight hours).

To assess the merits of the proposed approach, we provide the results of a comparison of the performances of the PHM system making full use of the Enhanced Particle Filtering strategy detailed in section 4, with respect to the results obtainable through the framework presented by authors in (De Martin, Jacazio, & Vachtsevanos, 2016), which did not include the noise compensation for long-term prediction nor the periodical check through on-ground measurements. For this example, we focus on the magnets degradation and its noisy feature. In Fig. 12, we compare the $\alpha-\lambda$ analysis of the Enhanced Particle Filter with that of the more traditional one. Due to the noisiness of the feature and the lack of the integration of the more precise information coming from on-ground tests, the old system converge to the real RUL extremely late in the fault development, providing a prognostic horizon of 24 hours, an average RA of 26.3% and a CRA of 34.76%.
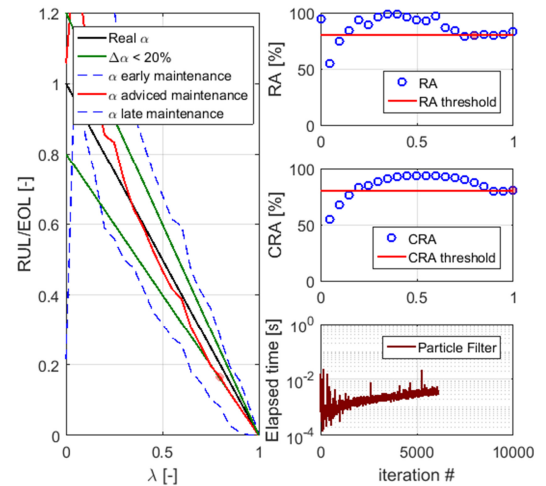


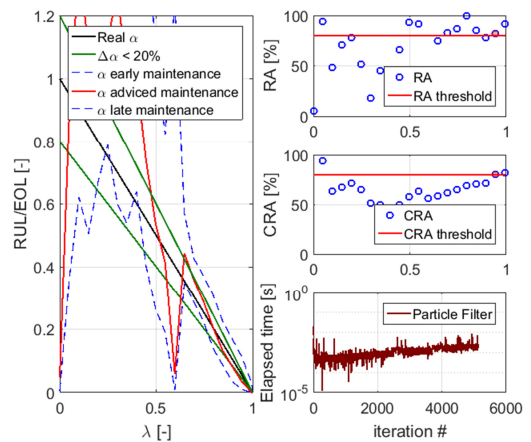Figure 10. Prognostic performance for wear in the mechanical transmission



Figure 9. Prognostic performances for magnets degradation



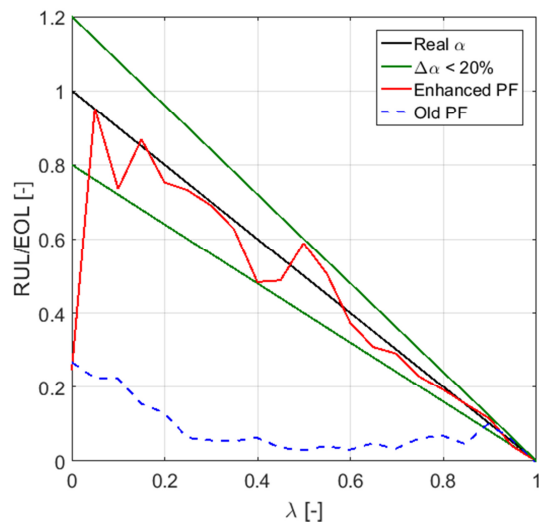Figure 11. Prognostic performance for wear in the rod-end

Figure 12. $\alpha$–$\lambda$ analysis for different PF frameworks

## 7. CONCLUSIONS

The paper at first presented the major issues to be faced while designing a PHM system for flight control actuators, highlighting the possible effects of the highly-varying operative conditions and the lack of dedicated sensors on prognostic applications. To address these issues, we proposed the combined use of data obtained during flight and during dedicated pre-flight checks, designed to highlight the effects of the degradation. An enhanced version of particle filtering framework for prognosis able to exploit this scheme has been introduced, discussed and hence applied to EMAs for flight control. The routines for fault detection and failure prognosis have been described, while their performances discussed through state of the art metrics. Finally, the benefits of the novel prognostic scheme have been highlighted through comparison with results obtainable through previously published methods. The presented approach lacks of any experimental confirmation, that will represent the most significant effort in continuing the research program. Activities in this subject are already planned and a dedicated high-performance test bench has been prepared. Moreover, the performances of the presented algorithm depends on the availability and frequency of the pre/post flight data and might by less suitable for long-range applications. Although defined for flight control applications, the approach of combining features obtained during normal operation with other measured in semi-controlled condition is easily extendable to other systems or application fields.

## ACKNOWLEDGEMENTS

## REFERENCES

Archard, J.F. (1953) Contact and rubbing of flat surface. *Journal of Applied Phisics* 24, pp. 981-988.

Arulampalam, S., Maskell, S., Gordon, and Clapp, N. J.(2002) A Tutorial on Particle Filters for On-line Non-linear/Non-Gaussian Bayesian Tracking, *IEEE Trans. on Signal Processing*, Vol. 50 (2) pp. 174-188.

Balaban, E., Saxena A, Goebel, K., Byington, C.S., Watson, M., Bharadwaj, S., and Smith M. (2009) Experimental data collection and modeling for nominal and fault conditions on electro-mechanical actuators, *Annual Conference of the Prognostics and Health Management Society*, September 27-October 1, San Diego, CA, USA.

Balaban, E., Saxena, A., Narasimhan, S., Roychoudhury, I., Gobel, K., Koopmans, M. (2010) Airborne electro-mechanical actuator test stand for development of prognostic health management systems, *Annual Conference of the Prognostics and Health Management Society*, October 10-16, Portland, OR, USA.

Bishop, C.M. (2009) Pattern recognition and machine learning, Springer.

Belmonte, D., Dalla Vedova, M.D.L., and Maggiore, P. (2015). New prognostic method based on spectral analysis techniques dealing with motor static eccentricity for aerospace electromechanical actuators, WSEAS Transactions on Systems 14.

Brown, D., Abbas, M., Ginart, A., Ali, I., Kalgren, P., and Vachtsevanos G. (2010). Turn-off time as a precursor for gate bipolar transistor latch-up faults in electric motor drives, *Annual Conference of the Prognostics and Health Management Society*, October 10-16, Portland, OR, USA.

Brown, D.W., Georgoulas, G., Bole, B., Pei, H.L., Orchard, M., Tang, L., Saha B., Saxena, A., Goebel, K., and Vachtsevanos G. (2009). Prognostics enhanced reconfigurable control of electro-mechanical actuators, *Annual Conference of the Prognostics and Health Management Society*, September 27-October 1, San Diego, CA.

Celaya, J.R., Saxena, A., Wysocki, P., Saha, S., & Goebel, K. (2010). Towards Prognostics of Power MOSFET. *Annual Conference of the Prognostics and Health Management Society*, October 10-16, Portland, OR, USA.

Christmann M., Seemann, S. and Janker, P. (2010). Innovative approaches to electromechanical flight control actuators and system, *Recent Advances in Aerospace Actuation Systems and Components*, May 5-7, Touluse, France.

Derrien, J., Tieys, P.,Senegas, D., and Todeschi, M. (2011). EMA Aileron COVADIS development. *SAE Technical paper*, 2011-01-2729.

De Martin, A., Jacazio, G., and Vachtsevanos, G. (2016) Anomaly detection and prognosis for primary flight control EMAs, *3rd European Conference of the Prognostics and Health Management Society*, July 5-8, Bilbao, Spain.

De Martin, A., Jacazio, G., Vachtsevanos, G. (2017) Windings fault detection and prognosis in electro-mechanical flight control actuators operating in active-active configuration, *International Journal of Prognostics and Health Management* 8(2).

Gokdere, L.U., Bogdanov, A., Chiu S. L., Keller, K. J. & Vian J. (2006) Adaptive control of actuator lifetime, *IEEE Aerospace Conference*, March 4-11.

Hanselman D. (2006) Brushless Permanent Magnet Design, UK, Magna Physics.

He, C., Li, J., and Vachtsevanos, G.J (2015) Prognostics and health management of an automated machining process, *Mathematical Problems in Engineering*.

Jacazio G., Maggiore P., Della Vedova M., Sorli M. (2010) Identification of precursors of servovalves failures for implementation of an effective prognostics, *Proceedings of the 4th International Conference on Recent Advances in Aerospace Actuation Systems and Components*, May 5th-7th, Toulouse, France.

Jensen, S.C., Jenney G.D. & Dawson D. (2000). Flight test experience with an electromechanical actuator on the F18 system research aircraft, *19th Digital Avionics System Conference* (page numbers), Edward, CA. doi: 10.1109/DASC.2000.886914.

Lessmeier C., Enge-Rosenblatt O., Bayer C., Zimmes D. (2014) Data acquisition and signal analysis from measured motor currents for defect detection in electromechanical drive systems, *European Conference of the Prognostics and Health Management Society*, July 8-10, Nantes, France.

Li, H., Ye, X., Chen, C., Vachtsevanos, G. (2014) A framework for model-based diagnostics and prognostics of switched-mode power supplies, Annual Conference of the Prognostics and Health Management Society, September 29 – October 2, Fort Worth, Texas.

Mornacchi, A., Vachtsevanos G., Jacazio G. (2015) Prognostics and health management of an electro-hydraulic servo actuator, Annual Conference of the PHM Society, October 18th-24th, Coronado, CAL, USA.

Mohan, N. (2003), First Course on Power Electronics and Drive, Minnessota, MNPERE.

Nandi, S., Toliyat H.A.& Li X. (2005) Condition monitoring and fault diagnosis of electrical motors – a review, *IEEE Transactions on Energy Conversion* 20, (4).

Nordin, M., Gallic, J., Gutman, P.O. (1997), New models for backlash and gear play, *International Journal od Adaptive Control and Signal Processing*, Vol. 11, pp. 49-63.

Orchard M (2007) *A Particle Filtering-based Framework for On-line Fault Diagnosis and Failure Prognosis*, PhD thesis, School of Electrical and Computer Engineering, Georgia Institute of Technology, Atlanta, GA, USA.

Pratt, R, (2000). *Flight control systems: practical issues in design and implementation,* U.K.: IET.

Recksieck, M. (2012). Advanced high-lift system architecture with distributed electrical flap, *2nd International Workshop on Aircraft Systems Technologies*, March 29-30, Hamburg, Germany.

Roemer, M.J., & Tang, L. (2015). Integrated vehicle health and fault contingency management for UAVs. In Valavanis K.P., Vachtsevanos G.J., *Handbook of Unmanned Aerial Vehicles*). Netherlands: Springer.

Ruoho S., Dlala E., and Arkkio A. (2007). Comparison of Demagnetization Models for Finite Element Analysis of Permanent-Magnet Synchronous Machines. IEEE Trans. Magn. 43, pp. 3964-3968.

Saxena A., Celaya J., Balaban E., Goebel K, Sasha B. & Schwabacher M. (2008) Metrics for evaluating performance of prognostic techniques, *International Conference on Prognostics and Health Management*, October 6th-9th, Denver, CO, USA.

Vachtsevanos G.J., Lewis F.L., Roemer M., Hess A., Wu B. (2006) *Intelligent Fault Diagnosis and Prognosis for Engineering Systems*, NY, John Wiley & Sons.

Van den Bossche, D. (2009) Servo Actuator Attachments, roller bearings vs PTFE lined spherical bearings. Presentation at 147th SAE A6 Meeting, San Antonio, Texas, October 25th – 30th 2009.

Wang L., Maré J.C., Fu Y. (2012) Investigation in the dynamic force equalization of dissimilar redundant actuation systems operating in active/active mode, 28th International Congress of the Aeronautical Sciences, Toulouse, France.